Anal. Chem. **2002,** *74,* 3819−3823

X-ray Absorption Fine Structure Combined with Fluorescence Spectrometry for Monitoring Trace Amounts of Lead Adsorption in the Environmental Conditions

Yasuo Izumi,*,† Fumitaka Kiyotaki,† Taketoshi Minato,† and Yoshimi Seida*,‡

Department of Environmental Chemistry and Engineering, Interdisciplinary Graduate School of Science and Engineering, Tokyo Institute of Technology, 4259 Nagatsuta, Midori-ku, Yokohama 226-8502, Japan, and Institute of Research and Innovation, 1201 Takada, Kashiwa 277-0861, Japan

The local structure of trace amounts of lead in an adsorbent matrix that contains a high concentration of iron and magnesium ($Mg_6Fe_2(OH)_{16}(CO_3)\cdot 3H_2O$) was successfully monitored by means of X-ray absorption fine structure spectroscopy combined with fluorescence spectrometry. A eutectic mixture of $PbCO_3$ and $Pb(OH)_2$ coagulated when Pb^{2+} was adsorbed from a 1.0 ppm aqueous solution, and in contrast, the major species was ion-exchanged Pb^{2+} in the case of adsorption from a 100 ppb aqueous solution. The difference was ascribed to the balance between the precipitation equilibrium for coagulation and the rate of the ion exchange reaction with surface hydroxyl groups.

X-ray absorption fine structure (XAFS) spectroscopy has become widely used to monitor the local structure of noncrystalline and heterogeneous/hybrid materials. Even with the state-of-the-art technology of synchrotron radiation and advanced X-ray detectors, there are still experimental difficulties measuring the absorption edge of trace amounts of an element in samples that contain a high concentration of heavy element(s).

We chose as an example a trace amount of lead adsorbed on $Mg_6Fe_2(OH)_{16}(CO_3)\cdot 3H_2O$ (adsorbent **1**). The adsorbent is one of the basic polyhydroxide compounds and exhibits a layered structure.[1] Several adsorbents containing aluminum are used for the removal of heavy metal elements. However, the risk of using aluminum in relation to the acceleration of Alzheimers disease cannot be excluded at the moment. Using a conventional XAFS measurement technique,[2] the X-ray fluorescence derived from a trace amount of lead is extremely weak relative to the background of the dominant scattered and emitted X-rays derived from the large quantities of iron and magnesium contained in the samples. This paper deals with a new analytical approach to the observed trace amount of lead and exhibits the speciation of adsorbed lead species.[3,4]

Lead, 1.0 wt %, was adsorbed on **1** from an aqueous Pb^{2+} solution of 1.0 ppm concentration. One of the most familiar environmental conditions relating to lead is the treatment of drinking water to suppress lead concentrations of 100−1000 ppb derived from soil contamination[5−7] or from pipes made of lead. A concentration of 1.0 ppm is the upper limit of Pb^{2+} concentration in the environment. The lower concentration was set to 100 ppb as the lower limit of Pb^{2+} in the environment. The removal from 100 ppb aqueous Pb^{2+} solution was tested up to lead contents of 0.12 and 0.30 wt % on adsorbent **1**.

It is a challenge to obtain local structural information for 0.12 wt % adsorbed lead from the 100 ppb aqueous solution. The Pb/Mg atomic ratio is 0.000 62. The edge jump for XAFS measurements in transmission mode[8] is 0.022 versus a total absorption of 4.0. The photon number ratio of Pb $L\alpha_1$ to Fe $K\alpha_1$ is 0.0058 in traditional fluorescence mode by using an ion chamber.[2] To enable measurements with a reasonable signal/background (S/B) ratio, a solid-state detector (SSD) may be ineffective.[9] An alternative measurement of the Pb K edge (88 005 eV) instead of the L_3 edge cannot give enough information about the bonding to oxygen atoms due to broadening effects,[10] and "double fluorescence X-rays" methods utilizing a Mn metal plate and Cr filter cannot selectively monitor the Pb $L\alpha_1$ signal.[13] In this work, XAFS combined with a high-energy-resolution fluorescence spectrometer[16−18] was applied to selectively monitor trace amounts of lead and obtain reliable spectra, free from the problems associated with

* Corresponding author: (e-mail) izumi@chemenv.titech.ac.jp.
† Tokyo Institute of Technology.
‡ Institute of Research and Innovation.

(1) Seida, Y.; Nakano, Y.; Nakamura, Y. *Water Res.* **2001**, *35*, 2341−2346.
(2) Lytle, F. W.; Greegor, R. B.; Sandstrom, D. R.; Marques, E. C.; Wong, J.; Spiro, C. L.; Huffman, G. P.; Huggins, F. E. *Nucl. Instrum. Methods Phys. Res.* **1984**, *226*, 542−548.
(3) Perera, W. N.; Hefter, G.; Sipos, P. M. *Inorg. Chem.* **2001**, *40*, 3974−3978.
(4) Fisher, E.; van den Berg, C. M. G. *Anal. Chem. Acta* **2001**, *432*, 11−20.
(5) Mortvedt, J. J. In *Fertilizers and Environment*; Rodriguez-Barrueco, C., Ed.; Kluwer Academic Publishers: Dordrecht, The Netherlands, 1996; pp 5−11.
(6) Gimeno-Garcia, E.; Andreu, V.; Boluda, R. In *Fertilizers and Environment*; Rodriguez-Barrueco, C., Ed.; Kluwer Academic Publishers: Dordrecht The Netherlands, 1996; pp 491−493.
(7) Ubavic, M.; Bogdanovic, D.; Cuvardic, M. In *Fertilizers and Environment*; Rodriguez-Barrueco, C., Ed.; Kluwer Academic Publishers: Dordrecht The Netherlands, 1996; pp 551−553.
(8) Rao, K. J.; Wong, J. *J. Chem. Phys.* **1984**, *81*, 4832−4843.
(9) The SSD should be operated in a detection mode with a high counting ratio to detect the weaker Pb $L\alpha_1$ in the presence of an excess of other X-rays. In this situation, photon counting loss phenomena and a lowering of the S/B ratio are inevitable.

10.1021/ac025550p CCC: $22.00 © 2002 American Chemical Society
Published on Web 06/17/2002

photon-counting losses or broadening effects at higher photon energies.

EXPERIMENTAL SECTION

Samples. Adsorbent **1** was synthesized using the procedure described in ref 1. Adsorbent **1** effectively adsorbed 100−1000 ppb Pb^{2+} at high flow rates (space velocity, 50−800 min^{-1}). The specific BET surface area of adsorbent **1** was 110 $m^2\ g^{-1}$. The distance between the nearest two layers was 7.79 Å based on the X-ray diffraction.

A 1.0 ppm lead(II) nitrate solution was adsorbed at a flow rate (space velocity) of 50 min^{-1} until the Pb content reached 1.0 wt % (Pb/Fe atomic ratio: 0.016), as checked by inductively coupled plasma (ICP) measurements. In a separate experiment, 100 ppb of lead(II) nitrate solution was interacted with adsorbent **1** at the same flow rate until the Pb contents reached 0.12 and 0.30 wt %, as checked by ICP. The Pb/Fe atomic ratio in the two specimens corresponds to 0.0019 and 0.0047, respectively. These samples were dried and pressed into disks (diameter, 20 mm).

Standard inorganic Pb^{II} compounds were used as received and diluted to 5.0 wt % Pb by mixing well with boron nitride using a mortar and pestle. The mixture was then pressed into disks (diameter, 20 mm). Ion-exchanged standard samples were prepared from Pb^{2+} aqueous solutions on three kinds of zeolites. The exchange ratio was 85.5 (NaY, JRC-Z-Y4.8, $Na_{58}Al_{58}Si_{134}O_{384}\cdot 240H_2O$), 6.3 (sodium mordenite, JRC-Z-M10, $Na_8Al_8Si_{40}O_{96}\cdot 24H_2O$), and 100% ($NH_4$-ZSM-5, PQ Corp., $Na_xAl_xSi_{96-x}O_{192}\cdot 16H_2O$ ($x < 27$)). The former two samples were distributed by the Catalysis Society of Japan. The case in which all the cation sites were exchanged with Pb^{2+} (substitute one Pb^{2+} for two Na^+ or NH_4^+) was defined as 100%.

X-ray Emission and Absorption Measurements. The X-ray measurements utilizing a fluorescence spectrometer were performed on the Undulator Beamline 10XU of SPring-8 (Sayo). The storage ring energy was 8.0 GeV, and the ring current was 100−72 mA. A Si(111) double crystal monochromator was used. A rhodium-coated double mirror set was inserted in the incident X-ray beam path in order to suppress X-ray higher harmonics.

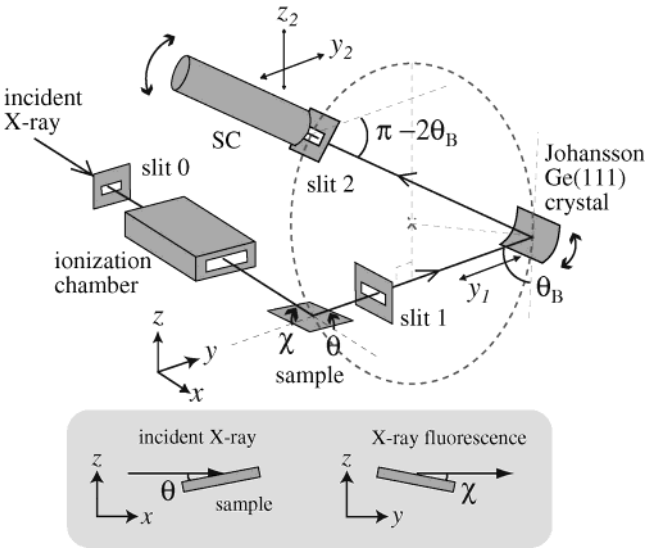

Figure 1. Configuration of the XAFS system combined with a fluorescence spectrometer.

The X-ray fluorescence from the sample was analyzed by a Rowland-type spectrometer (R = 220 mm) equipped with a Johansson-type cylindrically bent Ge(555) crystal (50 × 50 mm^2, Crismatec) and a scintillation counter (SC, Oken) (Figure 1).[17,18] The size of slit 0 was fixed at 1.0 × 1.0 mm^2 throughout the measurements. The samples were set in a plane slightly tilted from a horizontal plane. The Rowland circle was in the vertical plane. The top surface of sample holder was tilted toward the direction of the incident X-ray from the horizontal plane ($\theta = 6.0°$, Figure 1) and also toward the direction perpendicular to incident X-ray and in the same horizontal plane ($\chi = 7.0°$, Figure 1). The configuration in Figure 1 effectively focuses the divergence originating from the incident X-ray beam (polarized horizontally). The energy resolution was 1.1 eV at the Cu $K\alpha_1$ emission (8 keV), including the contribution of the beamline.[18]

The Pb $L\alpha_1$ emission spectrum was measured for Pb^{2+} adsorbed on **1** with the excitation energy set at 13 064.3 eV. The samples were at 290 K. The scan step was ∼0.9 eV, and 80 points were scanned between 10 535 and 10 605 eV. The dwell time of a point was 60 s. The photon counts at SC decrease as the energy resolution is improved. The energy resolution was lowered to 10.1 eV to obtain minimal photon counts (130 counts s^{-1}) at SC for 0.12 wt % Pb on adsorbent **1** by controlling the vertical size of slits 1 and 2 (Figure 1).[19] The emission energy of the Pb metal was calibrated to 10 551.5 eV.[20] The secondary fluorescence spectrometer was used to discriminate the minor Pb $L\alpha_1$ fluorescence from the scattered + emitted X-rays originating from the major Fe and Mg in the sample (Fe $K\alpha_1$ 6403.84, $K\alpha_2$ 6390.84, $K\beta_1$ 7057.98, Mg Kα 1253.60 eV). Similar optics have been reported in applications to improve the energy resolution of X-ray absorption near-edge structure (XANES) spectra[21,22] and in spin-[23] or site-selective

(10) Several K edge spectra at the higher energy (Ce 40 453−Pt 78 381 eV) were studied.[11] The mean free path λ of photoelectron at higher energy is expressed $\lambda = 1/(1/\lambda + m\Gamma_K/2\hbar k)$, where $\hbar$, m, k, Γ_K, are the Planck's constant, the mass, the wavenumber of the photoelectron, and the lifetime width of level K, respectively. The oscillation χ of EXAFS is expressed as the contributions of neighboring atoms i to absorbent $\chi(k) \propto \sum_i e^{-2R_i/\lambda} = \sum_i e^{-2R_i/\lambda} e^{-(R_i m/\hbar)(\Gamma K/k)}$. Thus, the lifetime broadening effects at higher energy should be emphasized by larger Γ_K for lead and a lower k value region.[11,12]

(11) Nishihata, Y.; Kamishima, O.; Kubozono, Y.; Maeda, H.; Emura, S. *J. Syncrotron Rad.* **1998**, *5*, 1007−1009.

(12) Uruga, T. at SPring-8, private communication.

(13) Secondary fluorescence X-rays, Mn $K\alpha_1$ (5898.75), $K\alpha_2$ (5887.65 eV), by the emission of Pb $L\alpha_1$ are monitored. The Mn K fluorescence yield is 0.314.[14] When a Cr filter (K absorption 5988.8 eV) is placed between the Mn metal plate and detector, mass absorption coefficients[15] are 62 and 471 for Mn $K\alpha_1$ and Fe $K\alpha_1$, respectively. The detection of Pb $L\alpha_1$ is not selective compared to the case of XAFS + fluorescence spectrometer.

(14) Tertian, R.; Claisse, F. *Principles of Quantitative X-ray Fluorescence Analysis*; Heyden: London, 1982.

(15) *International Tables for X-ray Crystallography*; MacGillavry, C. H., Rieck, G. D., Eds.; Reidel: Dordrecht, The Netherlands, 1985.

(16) Izumi, Y.; Kiyotaki, F.; Seida, Y. *J. Phys. Chem. B* **2002**, *106*, 1518−1520.

(17) Izumi, Y.; Oyanagi, H.; Nagamori, H. *Bull. Chem. Soc. Jpn.* **2000**, *73*, 2017−2023.

(18) Izumi, Y.; Kiyotaki, F.; Nagamori, H.; Minato, T. *J. Electron Spectrosc. Relat. Phenom.* **2001**, *119* (2/3), 193−199.

(19) Georgopoulos, P.; Knapp, G. S. *J. Appl. Crystallogr.* **1981**, *14*, 3−7.

(20) Bearden, J. A. *Rev. Mod. Phys.* **1967**, *39*, 78−124.

(21) Stojanoff, V.; Hamalainen, K.; Siddons, D. P.; Hastings, J. B.; Berman, L. E.; Cramer, S.; Smith, G. *Rev. Sci. Instrum.* **1992**, *63*, 1125−1127.

(22) Garcia, J.; Sanchez, M. C.; Subias, G.; Biasco, J.; Proietti, M. G. *J. Synchrotron Radiat.* **2001**, *8*, 892−894.

(23) Wang, X.; Grush, M. M.; Froeschner, A. G.; Cramer, S. P. *J. Synchrotron Radiat.* **1997**, *4*, 236−242.

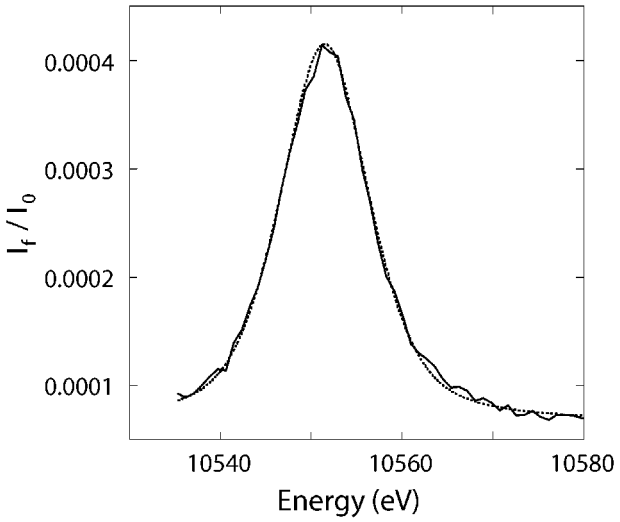

Figure 2. Pb $L\alpha_1$ emission spectrum for Pb^{2+} (0.12 wt %) on **1**. The solid line is the experimental data, and the dotted line is the fit with a pseudo-Voigt function. The intensity ratio of the Lorentzian and Gaussian components was fixed to 1:1.

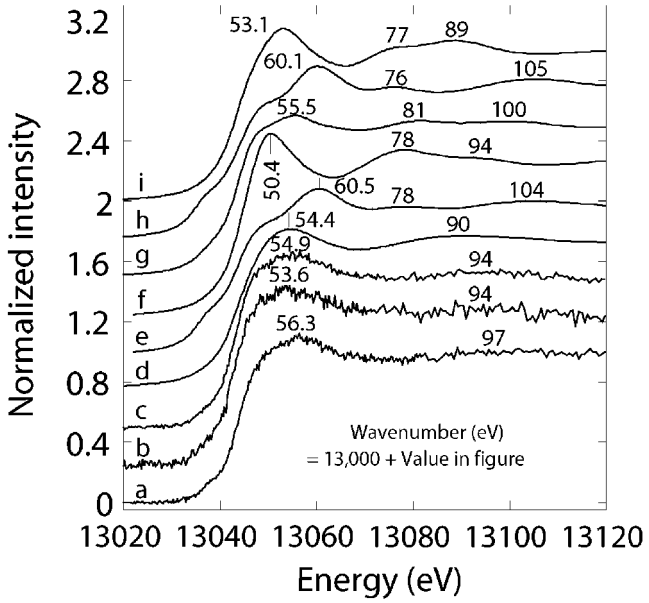

Figure 3. Normalized Pb L_3 edge XANES spectra for Pb^{2+} on **1** measured by utilizing a secondary fluorescence spectrometer (a−c). The Pb content was 1.0 wt % adsorbed from 1.0 ppm Pb^{2+} solution (a) and 0.30 (b) and 0.12 wt % Pb (c) from 100 ppb solution. Reference XANES spectra for PbY zeolite (d), PbO (e), $Pb(NO_3)_2$ (f), $2PbCO_3{\cdot}Pb(OH)_2$ (g), $Pb_6O_4(OH)_4$ (h), and $PbCO_3$ (i). (d−i) were measured in the conventional transmission mode.

XAFS.[24,25] In Figure 1, the Ge(555) bent crystal received a solid angle of 0.009 sr for the X-ray fluorescence emitted from the sample.

The fluorescence spectrometer was tuned to the peak of the Pb $L\alpha_1$ emission spectrum, and the Pb L_3 edge XAFS spectrum was measured. The scan steps were ∼0.3 and ∼0.6 eV for the edge and postedge regions, respectively. The Undulator gap and the piezoelement were optimized to maximize the X-ray beam flux at each data point. The dwell time of each data point was 40−120 s. The rising edge energy of the Pb metal was calibrated to 13 040.6 eV.[20]

Reference Pb L_3 edge XAFS spectra for standard Pb^{II} inorganic compounds and Pb^{2+} ion-exchanged zeolites were measured using a double crystal Si(311) monochromator in transmission mode at 290 K.

Analysis. Background subtraction of the raw XANES spectrum was performed by using a Victoreen parameter. The subtraction was not necessary in the case of XANES utilizing the fluorescence spectrometer. A smooth spline function was calculated in the postedge region, and then the spectrum was normalized at 13 095−13 115 eV. Derivative spectra of XANES utilizing the fluorescence spectrometer were smoothed using the locally weighted least-squares error method of KaleidaGraph 3.5.1 (Synergy Software).

RESULTS

Pb $L\alpha_1$ Emission Spectra. The Pb $L\alpha_1$ emission spectrum is depicted in Figure 2. The sample contained 0.12 wt % Pb adsorbed on **1** from a 100 ppb Pb^{2+} solution. The peak appeared at the same energy as for Pb metal (10 551.5 eV). The Pb $L\alpha_1$ emission spectra for other adsorbed Pb samples on adsorbent **1** and standard Pb^{II} compounds (not shown) were essentially the same with respect to peak energy position and peak width. The chemical shift on going from Pb^0 to Pb^{II} may be small or has an equivalent level of experimental error (<0.4 eV).[17,25] Therefore, site (state) selection of Pb^{II} was difficult in the case of Pb $L\alpha_1$. Furthermore, the core-hole lifetime width for Pb $L\alpha_1$ ($M_5 \rightarrow L_3$) is greater (the core-hole lifetime width of Pb L_3 is 5.81 eV[26]) than that of the K fluorescence lines of the first row of transition metal elements (1−2 eV; Mn $K\beta_1$, Fe $K\beta_1$, Cu $K\alpha_1$). Fortunately, only the Pb^{II} species are included in samples of this study.

The peak cannot be fit well using only Lorentzian or Gaussian functions. However, the peak can be fit well using a pseudo-Voigt function (a simple sum of Lorentzian and Gaussian functions)[27] (Figure 2, dotted line). The obtained full width at a half-maximum (fwhm) was 11.7 eV. Taking the core-hole lifetime width of Pb L_3 (5.81 eV) and a smaller M_5 into account, the energy resolution of the spectrometer was evaluated to be 10.1 eV, including the contribution of the beamline.

Pb L_3 Edge XANES Spectra. Normalized Pb L_3 edge XANES spectra are depicted in Figure 3. The rising edge positions are listed in Table 1. The rising edge for standard Pb^{II} inorganic compounds appeared within 13 043.4−13 044.9 eV, shifted by 2.8−4.3 eV toward higher energy from 13 040.6 eV for Pb^0. The rising edge for lead (0.12−1.0 wt %) adsorbed on **1** appeared within the range 13 042.9−13 044.2 eV, demonstrating that the adsorbed lead state was II and excluding the possibility of a lead site structure similar to $Pb^{IV}O_2$ or $Pb^{II,IV}{}_3O_4$. Based on the comparison of both the rising edge (Table 1) and inflection point energies (Figure 3), the spectrum for 1.0 wt % Pb on **1** (13 044.2 and 13 056.3 eV, respectively; Figure 3a) resembled only that for $2PbCO_3{\cdot}Pb(OH)_2$ (13 044.0 and 13 055.5 eV, respectively; g). Although the acetate

(24) Grush, M. M.; Christou, G.; Hamalainen, K.; Cramer, S. P. *J. Am. Chem. Soc.* **1995**, *117*, 5895−5896.
(25) Izumi, Y.; Nagamori, H. *Bull. Chem. Soc. Jpn.* **2000**, *73*, 1581−1587.
(26) Krause, M. O.; Oliver, J. H. *J. Phys. Chem. Ref. Data* **1979**, *8*, 329−338.
(27) Izumi, Y.; Glaser, T.; Rose, K.; McMaster, J.; Basu, P.; Enemark, J. H.; Hedman, B.; Hodgson, K. O.; Solomon, E. I. *J. Am. Chem. Soc.* **1999**, *121*, 10035−10046.

Table 1. Rising Edge Positions of Pb L_3 Edge Absorption for Pb^{2+} on **1** Measured Using a Fluorescence Spectrometer and for Standard Pb Compounds Measured in a Transmission Mode

sample	source	rising edge energy (eV)
Pb 1.0 wt % on **1**	from 1.0 ppm soln	13 044.2
Pb 0.30 wt % on **1**	from 100 ppb soln	13 042.9
Pb 0.12 wt % on **1**		13 043.1
PbY zeolite		13 043.4
PbO		13 043.8
$Pb(NO_3)_2$		13 044.9
$2PbCO_3{\cdot}Pb(OH)_2$		13 044.0
$Pb_6O_4(OH)_4$		13 044.2
$PbCO_3$		13 043.4
Pb metal		13 040.6

group does not exist in this adsorption system, Figure 3a resembled also that for $Pb(CH_3CO_2)_2{\cdot}3H_2O$ (not shown), suggesting the similarity of lead site structure to the case of $Pb(CH_3CO_2)_2{\cdot}3H_2O$. The samples of 0.30 and 0.12 wt % Pb on **1** were both prepared from 100 ppb Pb^{2+} solution, and the two spectra (b) and (c) resembled each other. The rising edge position and the inflection point shifted by 1.1−1.3 and 1.4−2.7 eV, respectively, toward lower energy on going from the Pb 1.0 wt % sample to the 0.30−0.12 wt % samples. Based on the comparison of both rising edge and the inflection point energies, these two spectra (13 043.0 ± 0.1 and 13 054.3 ± 0.7 eV, respectively) resembled only that for PbY (13 043.4 and 13 054.4 eV, respectively; d). The XANES spectra for lead mordenite and Pb-ZSM-5 were also measured (not shown). They were very similar to the spectrum for PbY (Figure 3d).

The above comparisons, based on the rising edge and the inflection point energies, can be rationalized by the comparison of spectrum patterns in the whole energy range of Figure 3. The edge regions of PbO, $Pb(NO_3)_2$ and $Pb_6O_4(OH)_4$ (Figure 3e, f, and h) were entirely different from those for adsorbed lead (a−c). Two postedge peaks appeared for $PbCO_3$ (i), which were relatively intense compared to the weak, flat postedge features in (a−c). No significant peaks in the postedge region were observed in (d), and (g), either. The very weak, broad peak at 13 097 eV of (a) corresponded to that at 13 100 eV in (g). A postedge broad, weak peak appeared at 13 094 eV for Pb 0.30 and 0.12 wt % (b and c). The energy position was similar to the case of PbY (13 090 eV, d) rather than that of $2PbCO_3{\cdot}Pb(OH)_2$ (13 081 and 13 100 eV, g).

An unresolved shoulder peak was observed at 13 049 eV in Figure 3a−c. A similar peak was also observed for $2PbCO_3{\cdot}Pb(OH)_2$ (g). No shoulder peak appeared in this region for PbY (d). This difference is clearly visualized in the derivative plots of the normalized XANES spectra (Figure 4). Two split peaks were observed at 13 044.0 and 13 052.2 eV for $2PbCO_3{\cdot}Pb(OH)_2$ (Figure 4e), whereas single peak at 13 043.4 eV was observed for PbY (d). The signal-to-noise (S/N) ratio is worse in (a−c), but dispite this, a separated peak feature clearly exists at 13 052 eV in addition to a major peak (i.e., the rising edge) at 13 042.9−13 044.2 eV in (a−c).

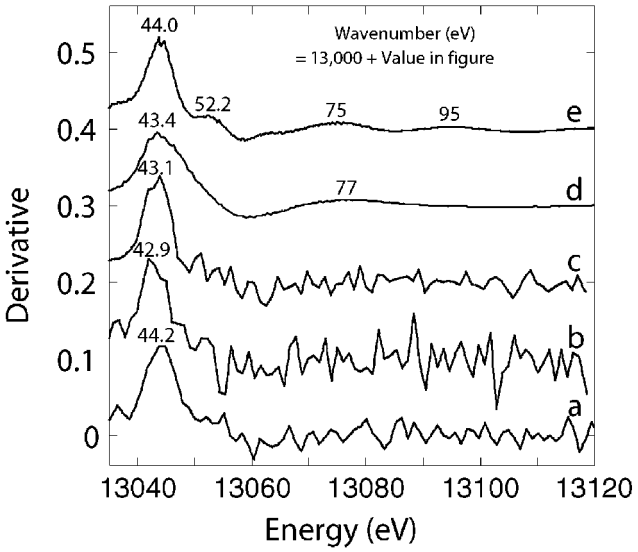

Figure 4. Derivative of the normalized Pb L_3 edge XANES spectra in Figure 3. The Pb content was 1.0 wt % adsorbed from a 1.0 ppm Pb^{2+} solution (a) and 0.30 (b) and 0.12 wt % Pb (c) from a 100 ppb solution. The reference derivatives are from PbY zeolite (d) and $2PbCO_3Pb(OH)_2$(e).

In summary, most of the Pb^{2+} coagulated as a eutectic mixture[28] of $PbCO_3$ and $Pb(OH)_2$ on **1** in the case of a 1.0 ppm solution. The formations of pure $PbCO_3$ by the reaction with intercalated/dissolved carbonate or pure $Pb_6O_4(OH)_4$ by a reaction with surface hydroxyl groups should be negligible. In contrast, in the case of the 100 ppb solution, the major lead phase was ion-exchanged Pb^{2+} via the surface reaction $OH + Pb^{2+} \rightarrow OPb^+ + H^+$. A shoulder peak at 13 049 eV suggests a minor contribution from coagulated eutectic mixture of $PbCO_3$ and $Pb(OH)_2$ on **1**.

DISCUSSION

By analyzing the X-ray fluorescence emitted from **1** containing trace amounts (0.12−1.0 wt %) of lead, the Pb $L\alpha_1$ signal was selectively monitored using an energy resolution of 10.1 eV. This energy resolution was good enough to discriminate the weaker Pb $L\alpha_1$ signal (10 551.5 eV) among dominant Fe $K\alpha_1$, $K\alpha_2$, $K\beta_1$, Mg $K\alpha$, and scattered X-rays (incident X-ray beam energy for excitation 13 064.3 eV).

Our methodology to selectively measure XANES utilizes a part of X-ray fluorescence directed to Johansson-type bent crystal (50 × 50 mm^2) among the solid angle of 2π from the sample surface, leading to a relatively low S/N ratio of XANES data. On the other hand, X-ray fluorescence collected at SC (Figure 1) was essentially all due to lead and background signal was negligible, leading to an extremely high S/B ratio.

In the case of goethite, an ion exchange mechanism was proposed for the lead removal.[29] The proposed ion exchange in the case of **1** proceeds as in eq A. If we assume the apparent density of **1** to be 0.5 g cm^{-3}, the concentration of Pb^{2+} to be 100−1000 ppb in the test solution, and a flow rate (space velocity) of 50 min^{-1}, it will take 4.5−45 days for the molar ratio of adsorbed

(28) Wells, A. F. *Structural Inorganic Chemistry*, 5th ed.; Clarendon Press: Oxford, U.K., 1984; p 628.
(29) Forbes, E. A.; Posner, A. M.; Quirk, J. P. *J. Soil. Sci.* **1976**, *27*, 154−156.

$$[Mg_3Fe(OH)_8]^+ + Pb^{2+} \rightarrow [Mg_3Fe(OPb)(OH)_7]^{2+} + H^+ \quad (A)$$

$Pb^{2+}/[Mg_3Fe(OH)_8]^+$ to reach unity. Step A is faster;[1,30] i.e. the ion exchange rate is essentially determined by diffusion. The rate can be compared to the coagulation rate in the proximity of **1** for an acidic Pb^{2+} solution (pH value, 3−5.5).

$$Pb^{2+} + nCO_3^{2-} + 2(1-n)OH^- \rightleftarrows nPbCO_3 \cdot (1-n)Pb(OH)_2 \quad (B)$$

The coagulation was proposed to proceed by the buffering effects of the basic surface of **1** (Figure 5). The pH value in the proximity of **1** becomes 7−8 due to the effect of hydroxyl groups of the adsorbent and coagulant chemicals released through a slight dissolution of the adsorbent during the buffering.[31,32]

For the adsorption from 1.0 ppm aqueous Pb^{2+} solution, $nPbCO_3 \cdot (1-n)Pb(OH)_2$ coagulated at a basic pH. Only the lead species similar to $2PbCO_3 \cdot Pb(OH)_2$ were detected by XANES, utilizing a fluorescence spectrometer (Figure 3a). The number of free Pb^{2+} ions that were able to access to the surface hydroxyl groups should be negligible.

In the case when the concentration in aqueous solution decreased from 1.0 ppm to 100 ppb, the equilibrium of coagulation shifted to the left-hand side of eq B. The ratio of the free Pb^{2+} ions in solution dramatically increased, and thus, the ion exchange reaction dominantly proceeded (eq A). Hence, the major species of ion-exchanged Pb^{2+} (right-hand side of step A) and the minor phase of the coagulated eutectic mixture of $Pb(CO_3)$ and $Pb(OH)_2$ (right-hand side of step B) were detected by means of XANES by utilizing a fluorescence spectrometer (Figure 3b and c).

The lead removal by adsorbent **1** is efficient in the range of flow rates (space velocity) of 50−800 min^{-1}, where a major part of lead ion cannot be trapped by activated carbon. In this range of flow rates, the concentration of Pb^{2+} solution was found to determine the kind of adsorbed lead species: eutectic mixture coagulation of $Pb(CO_3)$ and $Pb(OH)_2$ at higher concentrations (1.0 ppm) versus ion-exchanged Pb^{2+} with surface hydroxyl groups at lower concentrations (100 ppb).

This method combining XAFS with fluorescence spectrometry can be applied to perform a systematic survey of the removal process of dilute toxic elements, e.g., Cr, Cu, Zn, As, Cd, or Hg. Quantitative estimation should be extended in future in combination with the theory of XANES and EXAFS. The ultimate advantage of this method is when the energies of the minor and major X-ray fluorescence are different by less than 100 eV. In this case, no other detection systems can selectively detect the minor X-ray fluorescence derived from trace amounts of an element. The setup we have achieved (Figure 1) can achieve this with an energy resolution of 0.3−10 eV.

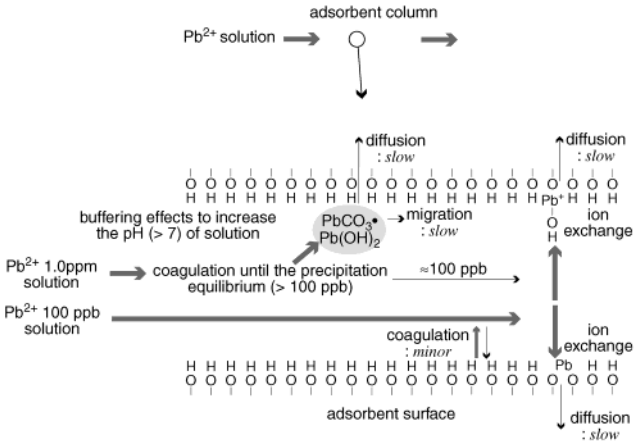

Figure 5. Pb^{2+} adsorption mechanism on **1** from Pb^{2+} 1.0 ppm and 100 ppb aqueous solutions.

CONCLUSIONS

The chemical state and local structure of 0.12 wt % Pb^{2+} were first determined by XAFS combined with fluorescence spectrometry. XANES is often utilized for speciation, and this paper extends the lower limit of concentration as small as 0.12 wt % lead in the presence of 17.35 wt % iron. The local structure was found to be dependent on the concentration of Pb^{2+} in the test aqueous solution: a eutectic mixture of $PbCO_3$ and $Pb(OH)_2$ and dominant ion-exchanged Pb^{2+} species in the case of adsorption from 1.0 ppm and 100 ppb Pb^{2+}, respectively. This difference can be explained by the balance between the precipitation equilibrium of the mixture $PbCO_3$ and $Pb(OH)_2$ and the ion exchange rate with the surface hydroxyl groups. The speciation of lead salts will be helpful in the design of materials for water treatment.

ACKNOWLEDGMENT

The experiments were performed under the approval of the SPring-8 Program Review Committee (2001A0022-NX-np and 2001B0004-CX-np). Y.I. expresses thanks for financial support from the Grant-in-Aid for Scientific Research from the Ministry of Education, Culture, Sports, Science, and Technology (13555230, 12740376), Yamada Science Foundation (2000), and Toray Science Foundation (98-3901).

Received for review January 28, 2002. Accepted May 6, 2002.

AC025550P

(30) Seida, Y.; Nakano, Y. *Water Res.* **2000**, *34*, 1487−1494.
(31) Seida, Y.; Nakano, Y. *J. Chem. Eng. Jpn.* **2001**, *37*, 906−911.
(32) Seida, Y.; Nakano, Y. *Water Res.* **2002**, *36*, 1306−1312.